XI International Conference on Computational Plasticity. Fundamentals and Applications
COMPLAS XI
E. Oñate, D.R.J. Owen, D. Peric and B. Suárez (Eds)

NON INTRUSIVE TECHNIQUE BASED ON DISCRETE ELEMENT APPROACH TO EXTRACT CRACK OPENING FROM 3D FINITE ELEMENT COMPUTATIONS

B. RICHARD, C. OLIVER, A. DELAPLACE AND F. RAGUENEAU

Laboratoire de Mcanique et Technologie (LMT)
ENS-Cachan/CNRS/Universit Paris 6/PRES UniverSud
61 Avenue du Prsident Wilson 94230 Cachan, France
e-mail: Benjamin.Richard@lmt.ens-cachan.fr
e-mail: Cecile.Oliver@lmt.ens-cachan.fr
e-mail: Arnaud.Delaplace@lmt.ens-cachan.fr
e-mail: Frederic.Ragueneau@lmt.ens-cachan.fr

Key words: Crack opening, discrete element, continuum damage mechanics, non-linear finite element, quasi-brittle material

Abstract. Closing the gap between damage and cracking is still nowadays an opened-question. This study aims at proposing a post-process technique to extract local information (crack openings) from continuous computations. In this paper, the approach is exposed and first results are discussed.

1 INTRODUCTION

When dealing with the behavior of plain concrete or reinforced concrete structures, the prediction of cracking remains a major issue. The effects of a crack on the durability of a structure are a major concern as long as the predictivity improvement for the numerical analysis is required. Not only the crack pattern but also crack features such as spacing, openings, rugosity or tortuosity have to be assessed at a member scale [1]. Two levels of analysis appear: the structure level and the crack level. Different approaches concerning structural modeling accounting for local nonlinear behaviors can be used to tackle the problems related to reinforced concrete structures subject to complex loading based on plasticity theories [2] or damage mechanics [3]. The use of such models needs the introduction of characteristic lengths to prevent the occurrence of spurious mesh dependency related to strain softening. Based on differential or integral nonlocal theories for example [4] or using viscosity approach [5], such characteristic lengths aim to smooth the discontinuity over a certain vicinity. The identification of the characteristic lengths is a major drawback when crack openings have to be quantified. Only a numerical post-treatment allows recovering the discontinuity features of a crack in terms of displacements jump [6].

Nevertheless, the problem remains unsolved in the case of multiple cracks as well as for composite materials such as reinforced concrete. An explicit description of a crack can be achieved using the discrete element methods [7]. The main physical mechanisms of quasi-brittle materials failure are recovered such as spatial correlation, crack tortuosity or scale effects. The mesh density needed for such modeling is nevertheless prohibitive to treat the case of industrial structures. More recent advances in numerical analysis of concrete structures have promoted the enhancement of finite element discretization by directly introducing material discontinuities in the finite element formulations. Based on shape functions finite elements kinematics enrichments [9] or nodal enhancements [10], such frameworks allow to deal with displacement jumps and singular stress fields close to the crack tip in case of strong discontinuity approach. For an industrial reinforced concrete structure such as nuclear power plant containment vessels for which hundreds of cracks may initiate and propagate, such numerical procedures would lead to excessive and prohibitive CPU time consumptions. The cyclic loadings including crack closing are also difficult to handle. The multiscale analysis introduces explicitly the two levels of interest: the structure level and the crack level. If a general agreement for employing finite element discretization at the macroscale is observed, the models employed at the local scale describing strong nonlinearities and discontinuities can be numerous. One can use refined meshing but homogeneous and continuous models [11], or introduce heterogeneities based on a continuous or a discrete approach. Such methods need coupling operators based on side-to-side modeling or overlapping domain [12]. An alternative procedure lies in the direct geographic coupling of two models based on a finite element discretization far from the zone of interest and a discrete modeling in the critical zone [13]. This kind of method needs to previously anticipate the localization of the part of the structure which will need a refine analysis with no possibility to extend the analysis without a complete remeshing. The purpose of the present study is therefore to propose a technique allowing the use of finite element models at a structural scale and a decoupled local analysis for some interesting zones for which a local information is needed. In this paper, first numerical results are shown and seem to be very encouraging for further works. In the first part, the theoretical framework of the proposed non-intrusive approach is exposed and, in a second part, numerical case studies are shown.

2 Combining finite and discrete element methods

The proposed decoupled strategy is obtained after a first analysis at macroscale, using here a finite element approach. Then, depending on the problem, a Region Of Interest (ROI) is defined, usually corresponding to the zones where the damage is developed. Note that if a sequential analysis is performed, the size of the ROI could evolve with the increasing of the loading. This ROI is then analyzed at the mesoscale, using here a discrete element approach, with the boundary conditions extracted from the macroscale computation applied on the non free surface of the ROI. The successive steps of the strategy are summarized in the following: (i) computation of the whole domain at the

macroscale, (ii) definition of the ROI to be analyzed at the mesoscale, (iii) definition of the coupling operators between both scales along the non free surface of the ROI and (iv) computation of the ROI at the mesoscale.

2.1 Definition of the Region OF Interest

The ROI that is reanalyzed at the mesoscale is a region where nonlinearities appear. In this contribution, we choose a fixed ROI (although we could have considered an evolving size of the region with respect to the evolution of the non linear region). Then, all the nonlinear domain obtained at the last step of the macroscale computation must be included in the ROI. This consideration allows avoiding any tricky coupling due to the nonlinear behavior through the ROI boundary. The boundary ∂R of the ROI is split into two parts: the free boundary ∂R_f and the boundary ∂R_u, where the boundary conditions obtained at macroscale will be applied. As soon as the ROI is defined, the coupling operators along ∂R_u between the two different scales are defined.

2.2 Coupling operators

The Dirichlet boundary conditions of the mesoscale computation are obtained from the macroscale computation, all along the non-free surfaces ∂R_u of the ROI. The natural way to transfer the displacement field from the macroscale to the mesoscale is to use the shape functions of the finite elements used at the macroscale. Then, the displacement $\bar{\mathbf{u}}_D(\mathbf{x}_D^0)$ at each nuclei $\mathbf{x}_D^0$ of the cells related to the discrete model along the ROI boundary are directly obtained with:

$$\bar{\mathbf{u}}_D(\mathbf{x}_D^0) = \sum_j \mathbf{N}_j(\mathbf{x}_D^0)\mathbf{u}_j \tag{1}$$

where $\mathbf{N}_j$ are the shape functions of the finite element model, $\mathbf{u}_j$ is the displacement vector computed at macroscale. The equilibrium of the ROI is naturally fulfilled if the same model is considered at macroscale and mesoscale. For two different models, one can obtain a slight gap from equilibrium, that should be estimated a posteriori. Next, we introduce an estimator of the gap between the continuous model and the discrete one.

2.3 Gap estimator

The advantage of this strategy, where the computation is performed twice (first at macroscale and second at mesoscale), is that an estimator of the gap between the two models is not limited to the ROI boundary but can be extended over the whole region. Then, one can distinguish the different areas where the models are more or less in agreement with each other. We propose a gap estimator based on the displacement fields obtained with the two models. As the displacement field at the mesoscale is only computed at the cells nuclei, we compute the gap estimator field at the cells nuclei, using the shape functions of the finite elements in order to compute the macroscale displacement.

The gap at the point $\mathbf{x}_D^0$ is:

$$\mathcal{E}(\mathbf{x}_D^0) = \frac{||\mathbf{u}_D(\mathbf{x}_D^0) - \sum_j \mathbf{N}_j(\mathbf{x}_D^0)\mathbf{u}_j||_2}{||\mathbf{u}_D(\mathbf{x}_D^0)||_2} \tag{2}$$

where $\mathbf{u}_D$ is the displacement field obtained at mesoscale. Note that:

$$\forall \mathbf{x}_D^0 \in \partial R_u, \qquad \mathcal{E}(\mathbf{x}_D^0) = 0$$

3 Continuum damage modeling for concrete

This section aims at giving an overview of the main features related to the concrete model used. A detailed description can be found in [14]. Formulating a constitutive model within the rigorous and consistent framework of the thermodynamically irreversible processes requires the definition of a state potential. This functional must be positive, convex and differentiable with respect to each variable. Moreover, this potential must lead to a satisfying description of the local mechanisms related to quasi-brittle materials such as the strong dissymmetry between the behaviors in tension and in compression, the inelastic strains and the unilateral effect. To split the difficulties, the cracked behavior will be assumed to be separated into two independent behaviors [15]: the hydro-static strain mechanisms and the frictional sliding. For the hydro-static strain mechanisms, only cracks opening and closing are considered. The frictional sliding is only treated on the deviatoric part of the strain and stress tensors. These considerations lead to a decomposition of the strain energy into two different parts, respectively due to the spherical and the deviatoric components. This feature is one of the key points for taking into account damage and sliding properly. A admissible state potential can be found (see [14]) and the positivity of the corresponding intrinsic dissipation can be shown (see [16]).

4 Discrete modeling

A particle-based discrete model is used for the fine crack description. With this approach, the material is described as a particle assembly. A crack is naturally obtained if a bond linking two particles breaks. A Voronoi tessellation is used, allowing an efficient and easy mesh generation. The particle nuclei are randomly generated on a grid [17] in order to control the boundary conditions. Cohesion forces can be equally represented either by springs at the interface of neighboring particles or by beams linking the nuclei of the particles. Euler-Bernoulli beams are chosen in the model used in this study. Then, four parameters have to be identified: the length ℓ_b, the cross section area A_b, the inertia I_b (or the adimensional parameter $\alpha = I_b/I_0$ where I_0 is the inertia of the equivalent circular section) and the elastic modulus E_b of the beam [18]. The first two parameters are prescribed by the mesh geometry and are different for each beam. The last two parameters are supposed equal for all beams and are identified in order to obtain the elastic properties of the material, E and ν, respectively the Young's modulus and the Poisson's ratio [19]. Note that if necessary, one can compute contact forces between unlinked particles, for

example for cyclic loading with crack opening and closing. The nonlinear behavior of the material is obtained by considering brittle behavior for the beams. The simplicity of this behavior is allowed because the model represents the material at a mesoscale, where just a simple phenomenon, a crack opening in mode I, is represented. The breaking threshold P_{ij} depends not only on the beam strain but also on the rotations of the particles (respectively i and j) linked by the beam. It is written as:

$$P_{ij}\left(\frac{\varepsilon_{ij}}{\varepsilon^{cr}}, \frac{\theta_{ij}}{\theta^{cr}}\right) > 1 \tag{3}$$

The critical strain ε^{cr} is identified by fitting the material tensile strength coming from basic mechanical tests. Then, the critical rotation θ^{cr} is identified by fitting the material compressive strength. Note that if the threshold depends only on the beam strains, the material compressive strength is overestimated by the model. With this simple beam behavior, one can obtain a reliable description of the material behavior, either for uniaxial loadings or biaxial ones [20]. Our study focuses (i) on a fine description of the crack pattern, and (ii) on the measurement of the crack opening. The crack pattern is defined as the common side of the particles initially linked by the breaking beams. The opening of the crack is computed by considering the relative displacement $(\mathbf{u}_j - \mathbf{u}_i)$ of the unlinked particles i and j. This approximation is justified by considering that the particles are rigid bodies and that the material is unloaded close to the crack lips. The measure of the opening between two particles i and j is projected on the normal $\mathbf{n}_{ij}$ of the local discontinuity, and is expressed as:

$$e_{ij} =< (\mathbf{u}_j - \mathbf{u}_i).\mathbf{n}_{ij} >_+ \tag{4}$$

where the dot stands for the scalar product.

5 Two-dimensional problem

We propose to test the proposed combining strategy on the single edge notched beam experimentally and numerically analyzed by [21, 22]. This test is particularly interesting because the loading ensures the rotation of the principal axes. Therefore, the main crack rotates with the principal directions making their propagation interesting to study. Such a crack pattern remains a major challenge for modeling assessments. We first focus on describing the finite element modeling realized. Second, the elastic response and the influence of the ROI size are analyzed and discussed. Last, we consider the crack propagation problem that requires a robust management of nonlinearities.

5.1 Finite element computation

The beam is 440 mm long, 100 mm height and 50 mm thick. A 5 mm notch is created on the top face, and a dissymmetric four-point bending test is carried out on the beam in order to ensure the rotation of the principal axes. To control the ratio between the loads,

a rigid trimmer has been modeled. A vertical displacement has been prescribed in such a way that the ratios $\frac{10}{11}$ and $\frac{1}{11}$ are ensured. The domain occupied by the concrete beam has been meshed by 394 three-node triangular elements. A coarse mesh has been chosen allowing to capture the global nonlinear phenomenon (damage field) with a reasonable computational cost. The local quantities of interest, such as stress singularities at the notch tip guiding the crack initiation and propagation, should be accounted for in the ROI using discrete modeling. The loading is controlled by displacement in order to improve the numerical robustness of the finite elements computations (in the nonlinear regime, in the following section). The concrete model used requires height material parameters: two related to the elasticity mechanism, four related to the isotropic damage mechanism and two related to the internal sliding. They have been identified with respect to the available experimental information (see [14]). They have been deduced from the experimental knowledge of the Young's modulus (40000 MPa), the compressive stress (37.5 MPa) and the tensile stress (2.70 MPa). The Poisson's ratio has been assumed to be equal to 0.2. Since the loading is purely monotonic, the material parameters related to the internal sliding mechanism do not play an important role. Therefore, no specific attention has been paid to identify them accurately. The characteristic length related to the non-local approach has been chosen equal to 5 mm, which ensures that two or three finite elements are included in the vicinity $\Omega(\mathbf{x}, l_c)$.

5.2 Elastic analysis

The proposed strategy is applied on the two following meshes. The first one is the mesh we use at the macroscale. The second one is the mesh we use at the mesoscale. 26 000 particules (78 000 dofs) are used. The meso model parameters are identified by ensuring the best force equilibrium when applying the boundary conditions computed from the macro computation. The gap estimator is shown on figure 1. The maximum is 60%, seemingly quite disappointing. The reason is obviously that a voluntary coarse mesh is used at the macroscale, that leads to a poor approximation of the displacement field at the macroscale. This effect is seen on the right hand side of figure 1, where a zoom is done around the notch, showing the 2000× amplified deformed shape of the macro- and meso-models. Local stress singularities due to cracks or notches conditioning crack initiation and propagation will be catched thanks to the meso discrete model. Using threshold on the gap estimator helps going deeper in the understanding of the numerical results. The first step is a lower thresholding at a level of 15% (figure 2-left). It is clear that the important gap is localized around the left side of the notch, where just one column of triangular elements are used. On the other hand, a upper thresholding at a level of 5% (figure 2-right) shows that the gap is lower almost everywhere on the ROI.

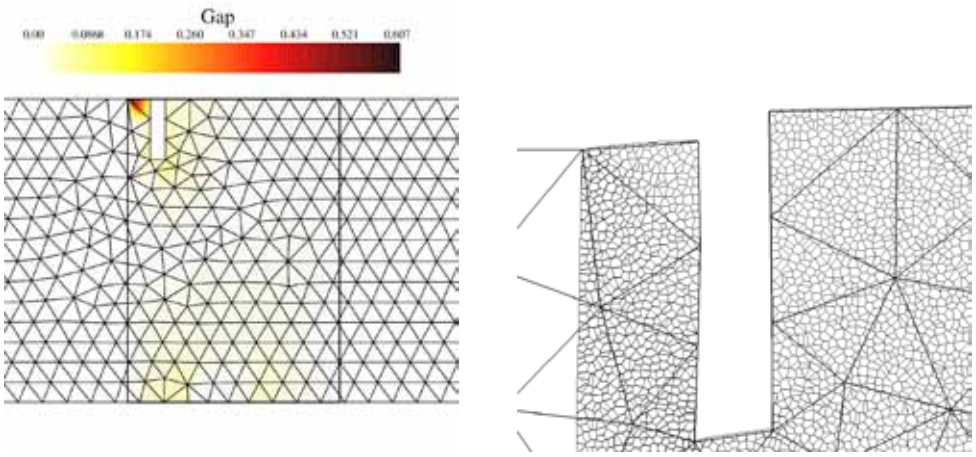

Figure 1: The gap estimator for the elastic loading on the Geers beam (left) and a zoom on the deformation (right).

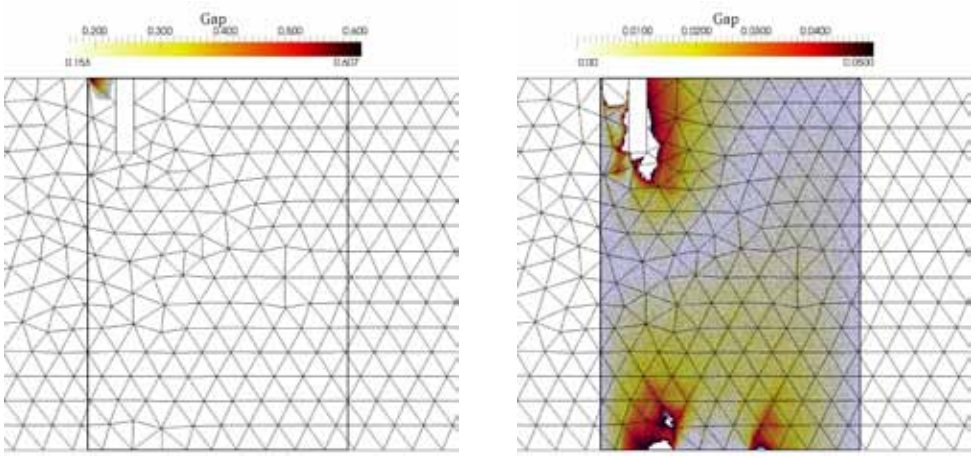

Figure 2: The gap with a lower threshold (15% left) and a upper one (5% right).

5.3 Nonlinear analysis

The nonlinear analysis is performed using the R_0-ROI. The main difference with the elastic analysis is that the macroscale resolution is now carried out by an incremental-iterative procedure, and different analyses at mesoscale should be done. An important point is that it is not necessary to perform mesoscale reanalysis for each macroscale computation step. The connectivity table between particles is initialized from the last discrete computation, and the boundary conditions are derived from the corresponding macroscale computation. For the 2D example considered in this paper, only three damage states (figure 3-top) for a total of 40 steps have been reanalyzed at mesoscale, leading to

the fine description of the cracking pattern in the center of the Geer's beam (figure 3-bottom). One can note the good agreement between the macroscale computation and the mesoscale one. As expected, it can be noticed that the mesoscale analysis obviously offers a finer description of the crack. In the final cracking pattern, one can distinguish a macrocrack starting from the notch as well as microcracks starting from the lower loading plate. It can be observed that the description of microcracking is not allowed only using macroscale analysis. Finally, the deformed configurations at the mesoscale and at the macroscale are presented in figure 4. Again a good agreement between both descriptions is obtained, but the crack opening is directly obtained only with the mesocale analysis.

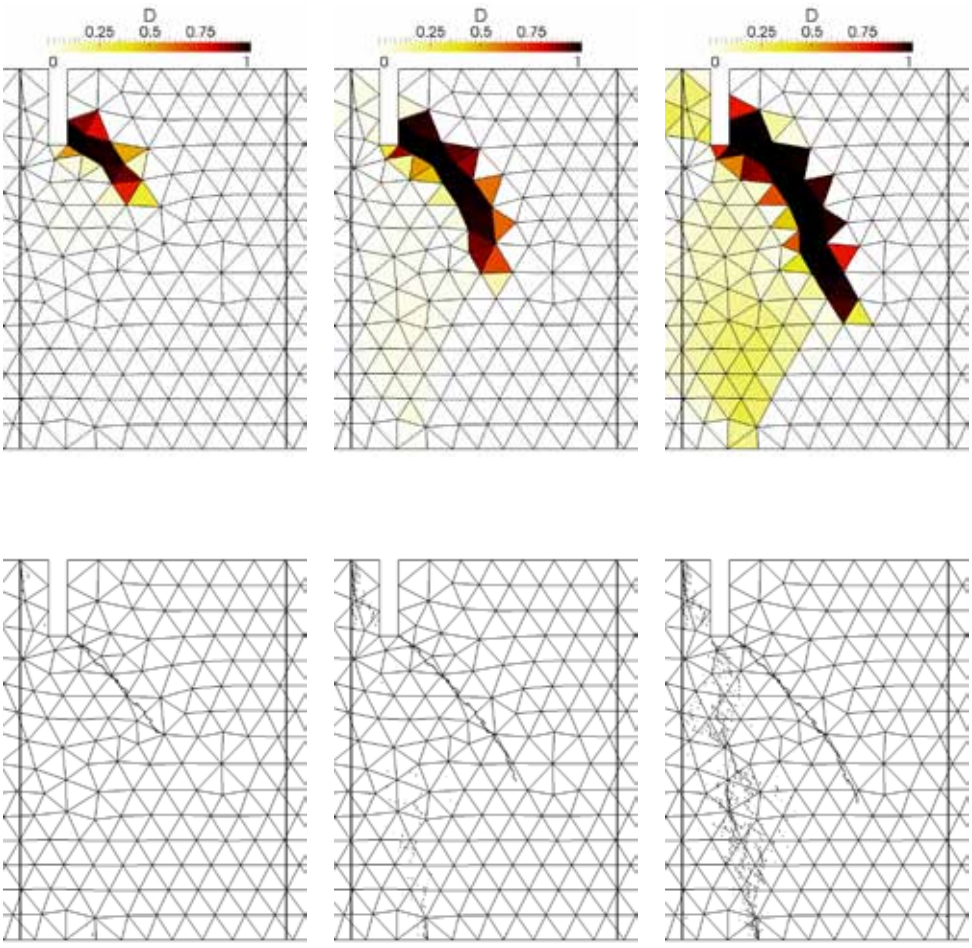

Figure 3: Damage maps and crack description obtained with discrete modeling.

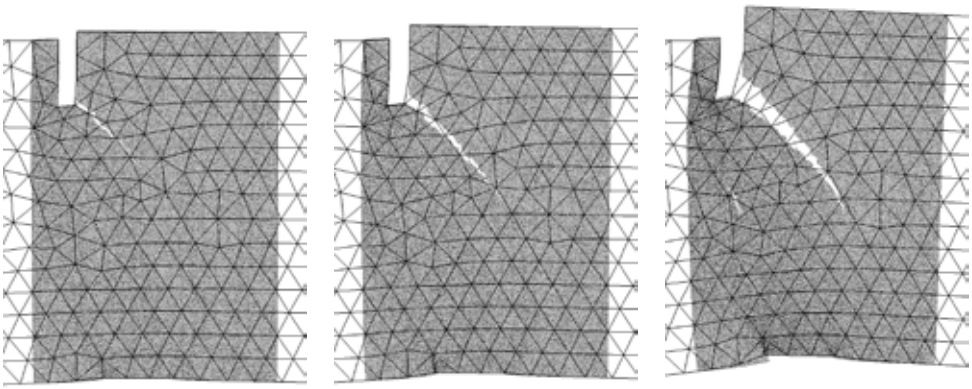

Figure 4: Deformation maps (×200).

6 Three-dimensional perpectives

We propose to apply the numerical strategy on a 3D problem. The protocol is strictly identical to the one used for the 2D problem. The only difference is that ∂R_u is now a surface compared to the line of the 2D case. We chose the PCT3D test proposed by Feist et al [23]. The feature of this test is a real 3D crack propagation, due to the asymmetry of the loading setup. The sample is a beam of 600 mm length, with a 180x180 mm square section, supported by two horizontal sleeves. A triangular notch is done in an angle of the mid section. The curves crack is obtained through an eccentric load.

Three damage states have been considered for the mesoscale reanalysis. These states are shown in figure 5 for the front face and in figure 6 in 3D, with the corresponding meso-scale results. Again, one can note the good agreement of the two analyses and the more realistic description of the crack at meso-scale. The value of the crack opening is given on the mesoscale cracking pattern (figure 6-right). Although the experimental values are not known all along the crack, one can note the satisfactory agreement of the numerical value (6.8×10^{-4} mm) with respect to the maximum experimental value (8×10^{-4} mm [23]) of the crack mouth opening displacement.

7 Conclusion

In this paper, an uncoupled numerical strategy dealing with a macroscale model and a mesoscale one is presented. The aim is to obtain a fine description of cracking (opening, length, tortuosity...) in certain regions of interest. The main concept is that a complete computation at macroscale is done, and a reanalysis at mesoscale using the boundary conditions computed at macroscale is carried out. The main features of the approach are the following: (i) the strategy is non intrusive and therefore does not require any

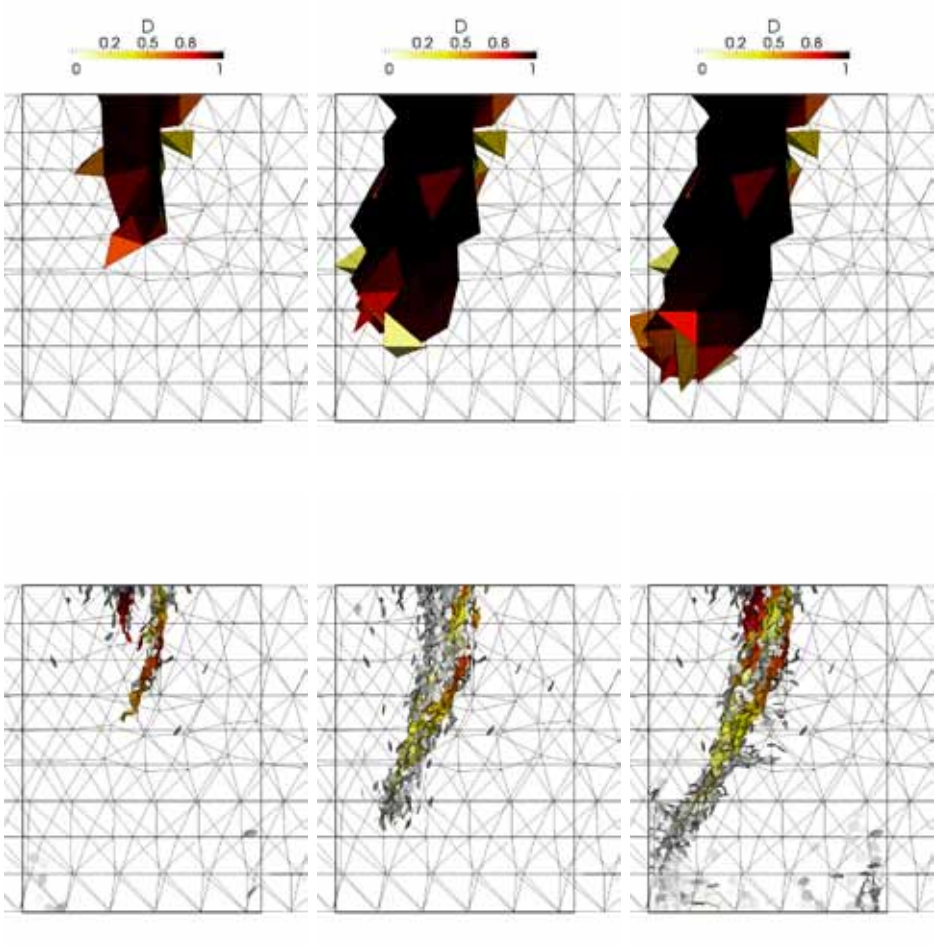

Figure 5: The damage patterns (top) obtained at macroscale and the correponding cracking pattern (bottom) obtained at mesoscale after the reanalyses.

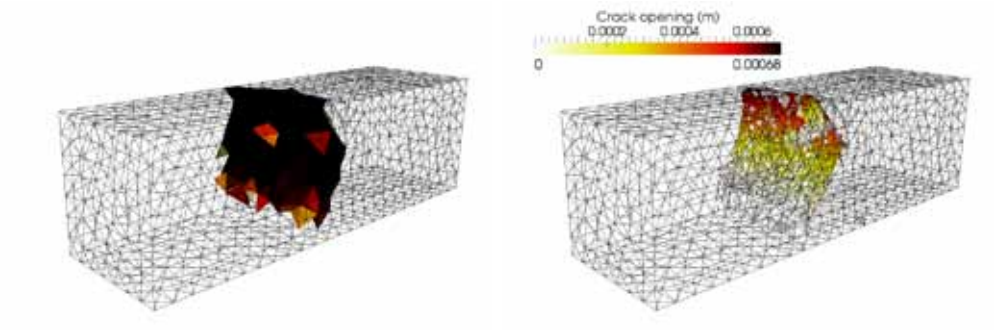

Figure 6: The 3D damage and cracking pattern obtained at the end of the loading.

modification of the computational codes, (ii) a gap estimator between both approaches can be estimated over the whole reanalyzed region and is not limited to the boundaries and (iii) because of the uncoupled resolution, the computations at the different scales can be naturally parallelized. The major drawback of the method is of course that the force equilibrium between the two levels is not verified since the a displacement based compatibility is used. Nevertheless, the different numerical results presented herein show that the obtained results are satisfactory. A further study dealing with this point is still under progress and will give quantitative results and discussions on this aspect.

REFERENCES

[1] Kozicki, J. and Tejchman, J. *Modeling of fracture processes using a novel lattice model. Granular Mat.* (2008) **10**(5):377–388.

[2] Dragon, A. and Mroz, Z. A continuum model for plastic-brittle behaviour of rock and concrete. *Int. J. Engn. Sci.* (1979) **17**:121–137.

[3] Mazars, J. Application de la mcanique de l'endommagement au comportement non linaire et la rupture du bton de structure, Universit Paris 6 (1984).

[4] Pijaudier-Cabot, G. and Bazant, Z. Nonlocal damage theory. *J. Eng. Mech. ASCE* (1987) **113**:1512–1533.

[5] Needleman, A. Material rate dependance and mesh sensitivity in localization problems. *Computer Methods in applied Mechanics and Engineering* (1988) **67**:69–85.

[6] Matallah, M. and La Borderie, C. and Maurel, O. A practical method to estimate crack openings in concrete structures. *International Journal for Numerical and Analytical Methods in Geomechanics* (2010) **34**:1615–1633.

[7] Cundall, P. A. and Strack, O. D. L. A discrete numerical model for granular assemblies. *Géotechnique* (1979) **29**:47–65.

[8] Bazant, Z.P. and Tabbara, M.R. and Kazemi, M.T. and Pijaudier-Cabot, G. Random particle model for fracture of aggregate and fibre composites. *Journal of Engineering Mechanics, ASCE* (1990) **116**(8):1686–1705.

[9] Belytschko, T. and Fish, J. and Engelman, B.E. A finite element with embedded localisation zones. *Computer Methods in applied Mechanics and Engineering* (1988) **70**:59–89.

[10] Moes, N. and Dolbow, J. and Belytschko, T. A Finite Element Method for Crack Growth Without Remeshing. *International Journal for Numerical Methods in Engineering* (1999) **46**:131–150.

[11] Feyel, F. and Chaboche, J.L. FE2 multiscale approach for modelling the elastoviscoplactic behaviour of long fibre SiC/Ti composite materials. *Computer Methods in applied Mechanics and Engineering* (2000) **183**:309–330.

[12] Gosselet, P. and Rey, C. Non-overlapping domain decomposition methods in structural mechanics. *Archives of Computational Methods in engeneering* (2006) **13**(4):515–572.

[13] Rousseau, J. and Frangin, E. and Marin, P. and Daudeville, L. Damage prediction in the vicinity of an impact on a concrete structure: a combined FEM/DEM approach. *Computers and Concrete* (2008) **5**(4):343–358.

[14] Richard, B. and Ragueneau, F. and Cremona, C. and Adelaide, L. Isotropic continuum damage mechanics for concrete under cyclic loading: stiffness recovery, inelastic strains and frictional sliding. *Engineering Fracture Mechanics* (2010) **77**:1203-1223.

[15] Pensée, V. and Kondo, D. and Dormieux, L. Micromechanical analysis of anisotropic damage in brittle materials. *J. Eng. Mech. ASCE* (2002) **128**:889–897.

[16] Adelaide, L. and Richard, B. and Ragueneau, F. and Cremona, C. Thermodynamical admissibility of a class of constitutive equation coupling elasticity, isotropic damage and internal sliding. *Comptes Rendu Mécanique* (2010) **338**:158–163.

[17] Moukarzel, C. and Herrmann, H. J. A vectorizable random lattice. *J. Stat. Phys.* (1992) **68**:911–923.

[18] Schlangen, E. and Garboczi, E. J Fracture Simulations of Concrete Using Lattice Models: Computational Aspects. *Eng. Fracture Mech.* (1997) **57**(2/3):319–332.

[19] Delaplace, A. and Desmorat, R. Discrete 3D model as complimentary numerical testing for anisotropic damage. *International Journal of Fracture* (2007) **148**:115–128.

[20] Delaplace, A. Tensile damage response from discrete element virtual testing. *Geomechanics and Geoengineering* (2009) **4**:79–89.

[21] Schlangen, E. Experimental and numerical analysis of fracture processes in concrete. *PhD thesis, Delft University of Technology, The Netherlands* (1993).

[22] Geers, M.G.D. and de Borst, F. and Peerlings, R.H.J. Damage and crack modeling in single-edge and double-edge notched concrete beams. *Engineering Fracture Mechanics* (2009) **65**(2/3):247–261.

[23] Feist, C. and Hostetter, G. Validation of 3D crack propagation in plain concrete. Part I: Experimental investigation - the PCT3D test. *Computers and Concrete* (2007) **4**(1):49–96.